Near-Threshold Fatigue Crack Path in Al Alloys

Jean PETIT

Laboratoire de Mécanique et de Physique des Matériaux - UMR CNRS n' 6617
ENSMA - Téléport 2 - B.P. 109 - 86960 Futuroscope Cedex - France

petitj@lmpm.ensma.fr

INTRODUCTION

Near-threshold fatigue crack propagation behavior of metallic alloys has been widely studied and documented during the last three decades. Several factors or parameters have been shown to play a major role [1,2,3]. Firstly, the microstructure effects have been shown to dominate the near-threshold regime and to widely influence the crack path. Secondly, comparative measurements of fatigue crack propagation rates in air and in high vacuum have demonstrated the existence of a detrimental effect of atmosphere environment for most of the metallic materials fatigued at room temperature this effect being much more accentuated in the near-threshold area; experiments conducted under controlled partial pressures of water vapor have clearly related the acceleration of the fatigue crack growth rate to the presence of moisture in the surrounding gaseous environment [4]. Thirdly, crack closure in the near-threshold area induces enhanced shielding effects which depend on the crack wake and hence on the crack path (plasticity, closure mismatch of rough surfaces, oxidation) [5].

This paper deals with a review on the role of microstructure and environment on the near-threshold fatigue crack propagation behavior in Aluminum alloys and particularly on Al-Zn-Mg alloys. Possible interactions of crack closure are uncoupled by considering data provided by tests with closure correction or without closure. Relations between crack paths and crack growth mechanisms are discussed on the basis of micrographic and microfractographic observations.

INTRINSIC CRACK PROPAGATION PATH

Intrinsic Transgranular Crack Propagation

As previously recommended by Wei *et al.* [6], because of the sensitivity to an aggressive environment (including ambient air) of fatigue crack propagation in metallic alloys, environment control is very important. An additional recommendation must be made for the use of effective data (i.e., including correction for crack closure as proposed by Elber [5]), if the experimental data are intended for use in correlating with theories of fatigue crack propagation.

A fundamental approach of the relation between the crack path and the microstructure has been conducted on single crystals and polycrystals of high purity Aluminum-Zinc-Magnesium alloys [4,9,10] and commercial 7xxx alloys [4,11,12]. Tests were performed in air and in high vacuum, at a frequency of 35 Hz, with a load ratio R = 0.1 or R= –1; closure correction were done using the compliance, and some tests were run at constant K_{max} in condition without closure [4].The intrinsic crack path (which means the path of a crack grown in high vacuum with closure correction or without closure) can be analyzed in accordance to three fundamental transgranular crack propagation regimes and one intergranular regime.

Three transgranular regimes have been identified as follows:

(i) Intrinsic Stage I has been identified on peak-aged Al-Zn-Mg single crystals (Figs 1 and 3). Typically, a crack grown in a single crystal plane pre-oriented for single slip will develop within a {111} plane inclined at an angle of 45° against the tensile axis (Fig. 1). This intrinsic regime is observed in microstructure favoring heterogeneous

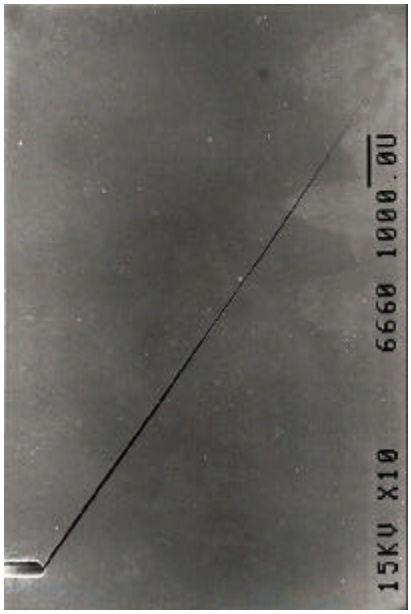

Figure 1. Stage I crack growth in high vacuum in a peak-aged single crystal of Al-4.5% wt Zn-1.25% wt Mg alloy preoriented for (111) slip (R=0.1, 35 Hz). Note: OU is equivalent to one micrometer.

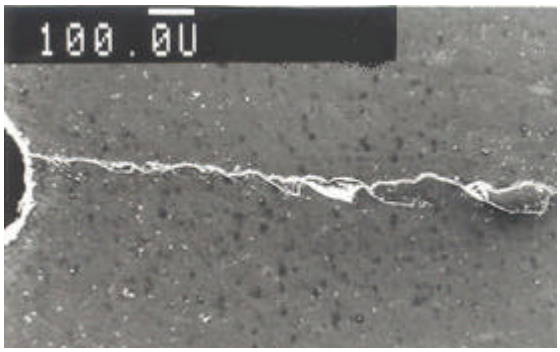

Figure 2. Stage II crack grown in high vacuum in an overaged single crystal of Al-4.5% wt Zn-1.25% wt Mg alloy pre-oriented for easy slip (R=0.1, 35 Hz).

deformation along a single slip system, as under- and peak-aged Al alloys containing fine and coherent GP zones. The stage I regime can also be operative in the initial grain

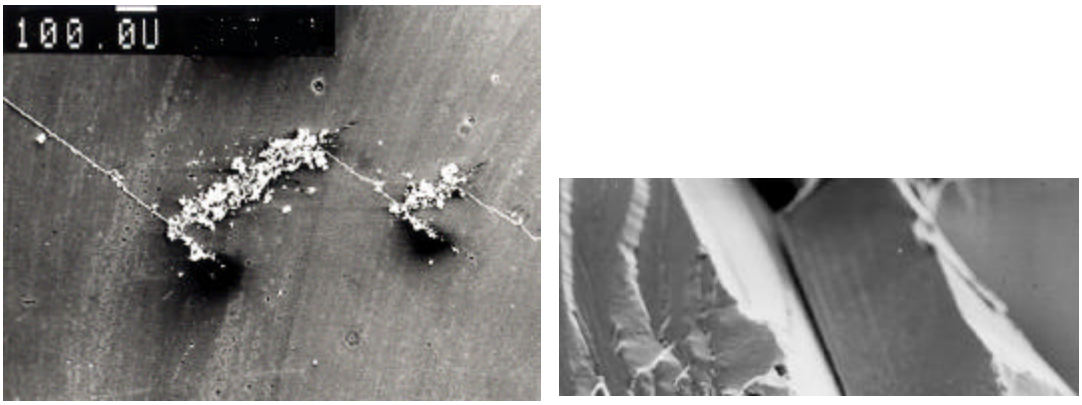

a) b)

Figure 3. Zig-zag stage I like crack grown in high vacuum (R=-1 and 35Hz) in an Al-Zn-Mg singlecrystal not oriented for easy slip (see intense wear associated to roughness induced closure): a) crack profile and b) crack surface.

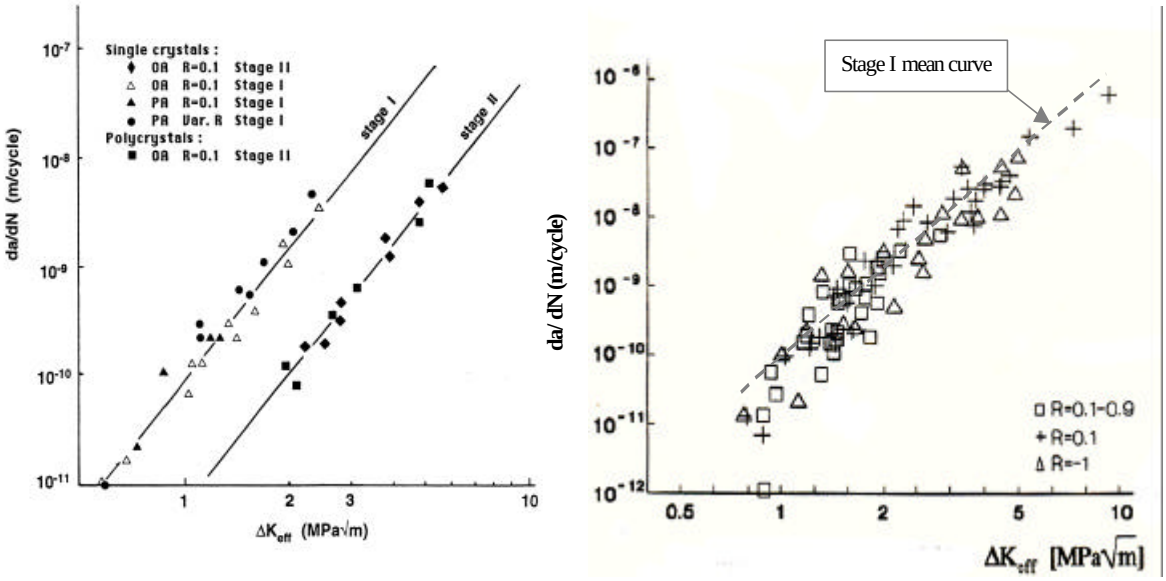

a) b)

Figure 4. Intrinsic crack propagation data in high vacuum of single crystals and polycrystals of Al-4.5% wt Zn-1.25% wt Mg alloy with closure corrected ΔK_{eff} values corresponding to mode I loading (R=0.1, 35 Hz). a) Pure stage I in single crystals oriented for easy slip and stage II in singlecrystals and polycrystals; b) Comparison of intrinsic data for pure stage I and zigzaging stage I in singlecrystals for different load ratios.

initial grain for a microcrack initiated at the surface of a polycrystal [11]. If the crystal or the grain is not well oriented for single slip, the crack will have a zigzag path following (111) planes of different orientations (Fig. 3a) and leading to a highly faceted crystallographic crack path which is not a pure stage I regime (Fig. 3b).

The pure intrinsic stage I propagation curve da/dN vs ΔK_{eff} for single crystal oriented for easy slip is drawn in Fig. 4a, and data in a similar diagram for zigzag stage I in not well oriented crystals are plotted in Fig. 4b. The scatter in the latter diagram can be attributed to the geometrical effect of crack branching and deviation on the stress intensity factor range [16]. However, all these data are consistent with a single intrinsic stage I regime as identified in Fig. 4a, with da/dN proportionnal to $(\Delta K_{eff})^4$. Figure 4b confirms that after closure correction there is no significant effect of the load ratio R.

(ii) **Intrinsic Stage II** corresponds to a crack developing in a plane normal to the load axis and resulting from an alternating slip mechanism on symmetric (111) slip systems as identified in overaged Al-Zn-Mg in single crystal pre-oriented for single slip (Fig. 2). In polycrystals (Fig. 5a) a very similar stage II is observed in the Paris regime. It is favored by microstructures with large and non-coherent precipitates such as overaged Al alloys which promote homogenous deformation and wavy slip. The intrinsic stage II propagation curve for the high purity Al-4.5% wt Zn-1.25% wt Mg alloy tested in high vacuum at R=0.1and 35 Hz is presented in Fig. 4a.

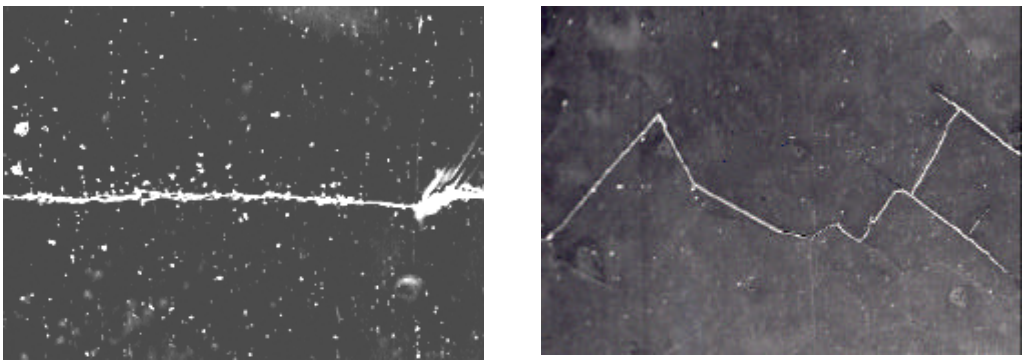

a) b)

Figure 5. Intrinsic crack path in high vacuum of polycrystals of Al-4.5% wt Zn-1.25% wt Mg alloy (R=0.1, 35 Hz): a) stage II crack in overaged condition and b) stage I like crack in peak-aged condition.

More generally, the intrinsic stage II regime for mode I opening is in accordance with a propagation law derived by Petit et al. [4,13] from the models initially proposed by Rice [14] and Weertman [15] :

$$(da/dN)_{intrinsic} = A/D_0^*(\Delta K_{I,eff}/E)^4 \quad (1)$$

where A is a dimensionless parameter, E the Young modulus and D_0* the critical cumulated displacement leading to rupture over a crack increment ahead of the crack tip and $\Delta K_{I,eff}$ is the effective range for the mode I stress intensity factor. It has been shown that this regime shows little sensitivity to the alloy composition, microstructure, grain size or yield stress; the growth rate is essentially dependent on the effective stress intensity range and on the Young modulus when comparing with other alloys as steels and Ti alloys.

(iii) **Intrinsic Stage I-Like** propagation corresponds to a crystallographic crack path which is observed in polycrystals in the near-threshold domain (Fig. 5b) or in the early stage of growth of naturally initiated small cracks [4,11]. This regime is favored by heterogeneous deformation along single slip systems within individual grains in microstructure containing fine and shareable precipitates such as GP zones in underaged Al alloys. The corresponding crack propagation curve is presented in Fig. 6 in comparison to the intrinsic stage I and stage II regimes. Crack branching or crack

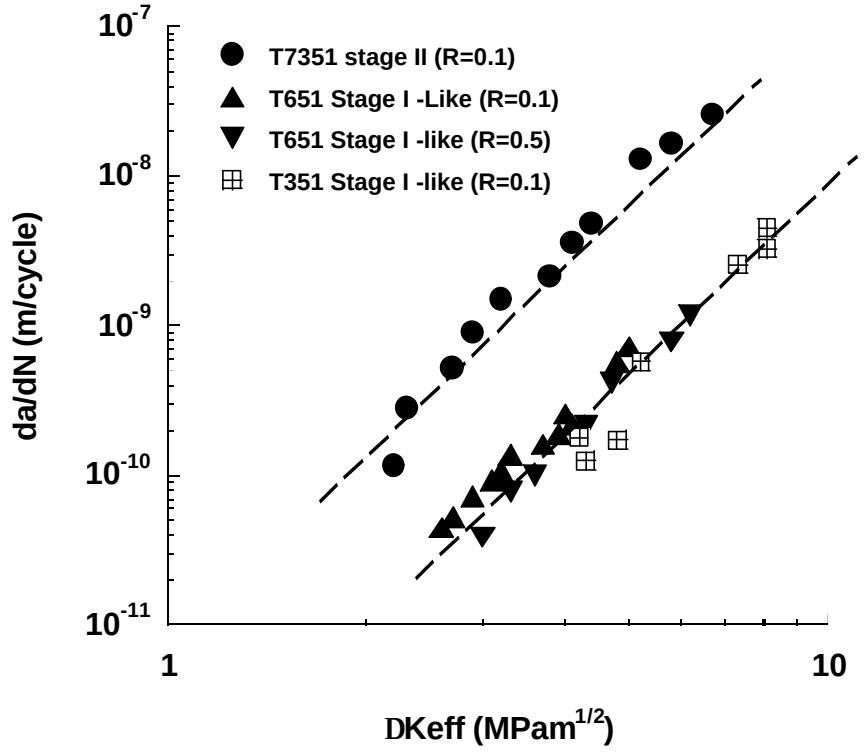

Figure 6. Comparison of intrinsic stage II and stage I like propagation regimes in a 7175 Aluminum alloy in three different aging conditions tested in high vacuum at 35 Hz.

.

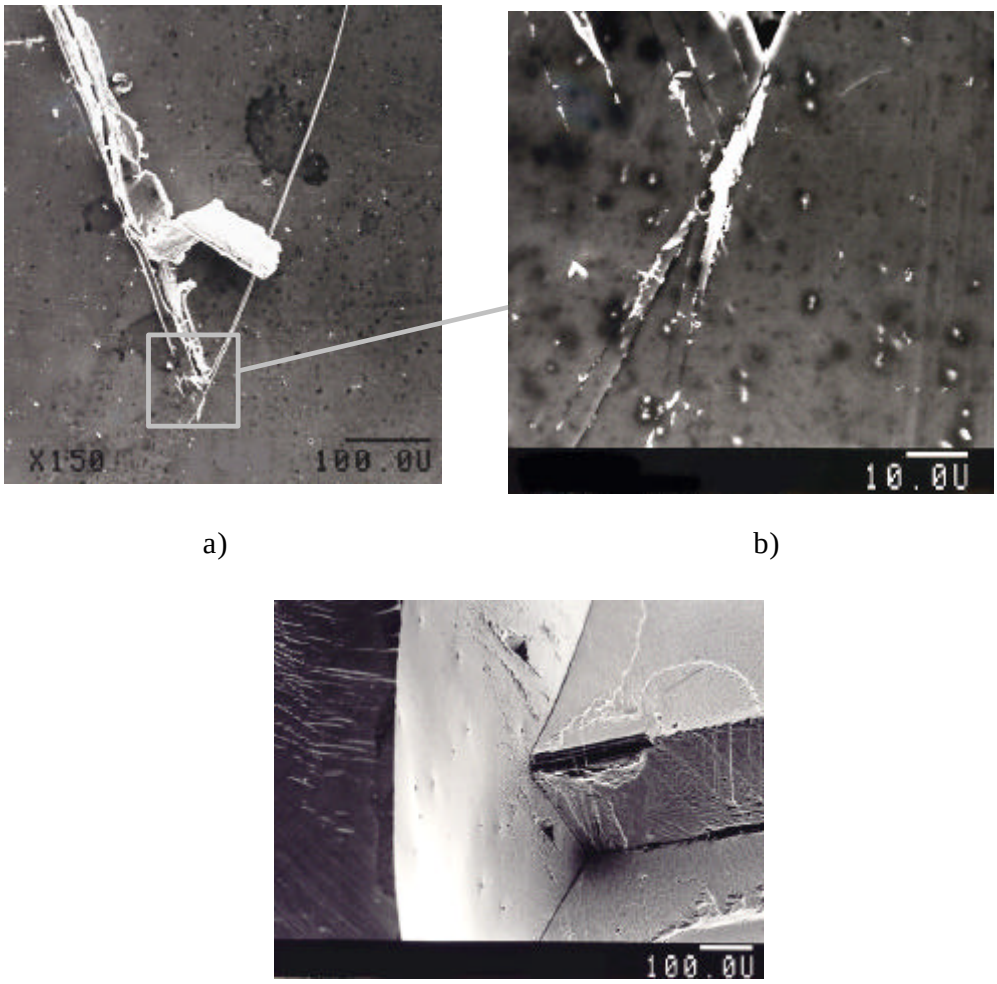

a) b)

c)

Figure 7. Barrier effect of a grain boundary for a stage I crack: a) grain boundary blockage of a stage I crack; b) initiation of a (111) slip system in the neighbor grain; c) fracture surface with a stage I crack on the left hand, a stage I like crack in the neighbor grain on the right hand, and a segment of intergranular crack in the grain boundary.

deviation mechanisms in single crystals have been shown to induce only small shielding effect on the stress intensity factor at the tip of the main crack (Fig. 3b). Consequently, the strong retardation effect in polycrystals must be mainly attributed to the barrier effect of grain boundaries [17] which results from the difficulty to generate a new slip system in the next grain (Fig. 7). This barrier effect has been shown more accentuated when the number of available slip systems is reduced as in Ti alloys [4] or drastically reduced when some additional slip systems can be activated as in the precipitate free zones in Al-Li alloys with Li addition higher than 2.5% [4].

Fracture Surface Morphology

As is shown in Fig. 1, stage I cracks are inclined at an angle of 45°C against the load axis in single crystals oriented for easy slip or are close to that angle in other cases (Fig. 3). Hence, they are submitted to a mixed mode of opening combining mode I (tension)

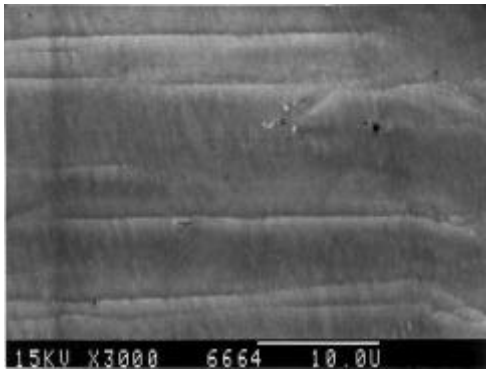

a)

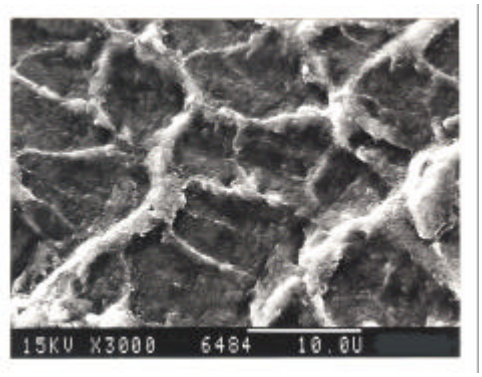

b)

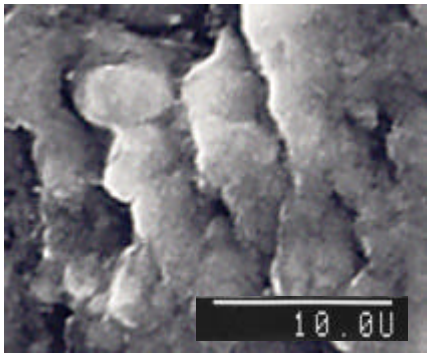

c)

Figure 8. Fracture surface morphology of a crack grown in high vacuum in a peak-aged single crystal of Al-Zn-Mg alloy: a) stage I crack in the near threshold domain (da/dN~ $1.5x10^{-11}$ m/cycle, ΔK_{eff} ~ 0.9 MPa$\sqrt{m}$); b) stage I crack near stageI/stage II transition (da/dN ~ 3.10^{-8} m/cycle,ΔK_{eff} ~ 4.2 MPa$\sqrt{m}$); c) stage II crack (da/dN ~ 10^{-8} m/cycle, ,ΔK_{eff} ~ 6 MPa$\sqrt{m}$).

and mode II (shearing). In peak-aged single crystals, PSB's developing along (111) slip plane favor a localization of the deformation in a wide stress range while in the overaged alloy the shearing mode is only predominant in the near-threshold condition (da/dN about 10^{-10} m/cycle). The surfaces of the stage I crack in the peak-aged alloy show very flat areas with long steps oriented in the crack propagation direction (Fig.

8a). At higher growth rates, the shearing mode is still dominating, but a contribution of the mode I of opening can be detected with the appearance of dimples corresponding to the size of dislocation cells generated by the tensile stress (Fig. 8b). At much higher stress intensity factor range and, hence faster da/dN, the crack propagation regime switches from stage I to Stage II when the mode I contribution becomes predominant. This transition in the propagation stage is reversible and a stage II crack may switch to the stage I regime when approaching the near-threshold conditions[4] . The surface morphology of stage II crack (Fig. 8c) presents a flat and uniform aspect only marked by ductile striations which spacing is of the same size as the dislocation cells in Fig. 8b. This kind of crack path has been associated to an alternating slip mechanism operating on symmetric slip systems simultaneous activated in this regime and particularly in air [18, 19]. In contrast to stage I like cracks, the path of stage II cracks shows little sensitivity to grain boundaries (no detectable barrier effect).

Intrinsic Intergranular Crack Path

Fatigue crack propagation tests were performed in Al-Zn-Mg bicrystals and polycrystals in high vacuum to examine the role of grain boundaries on the crack path and the associated fatigue crack propagation mechanism. An example of an intergranular crack grown in high vacuum in a bicrystal with a grain boundary not far from the normal crack

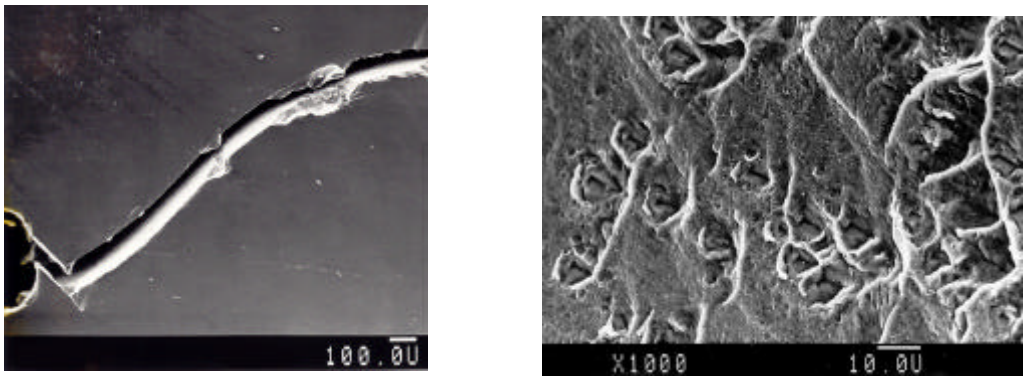

a) b)

Figure 9. Intergranular path of a crack grown in high vacuum in a bicrystal of high purity peak-aged Al-Zn-Mg alloy (R=0.1, 35Hz): a) crack profile; b) crack surface.

plane is given in Fig. 9a. After a crystallographic transgranular initiation stage, when the crack meets the grain boundary inclined at an angle not far from 45° against the load axis in this specimen, the easiest crack path appears to be the boundary for ΔK ranging about 5 to 6 MPa$\sqrt{m}$ (da/dN about 2 to $6x10^{-8}$ m/cycle). The crack surface in Fig. 9b reveals a flat surface essentially marked by traces of intergranular precipitates looking

like dimples. The intergranular crack propagation rate at 35 Hz is comparable to that of the transgranular intrinsic stage II crack. Comparable transgranular crack path are observed when a stage I like crack is grown in a polycrystal. These areas allow the link up of stage I cracks which develop in individual grains. As is illustrated in Fig. 7, a transgranular stage I crack has difficulty to cross over a grain boundary and the resulting crack arrest corresponds to the time (or number of cycles) required to build up a new slip system in the next grain. In addition, the initiation point of this new slip system is not exactly at the tip of the stage I crack grown in the first grain, and hence a segment of intercrystalline crack path is required to link up the first stage I crack to the new one which develops along one or more (111) planes having other orientations in the next grain (see Fig. 7c). In the same manner, a stage I-like crack grown in a polycrystal will meet various grain orientation and finally this results in a rough crack path mixing predominant transgranular crystallographic facets and intergranular areas (Fig. 10).

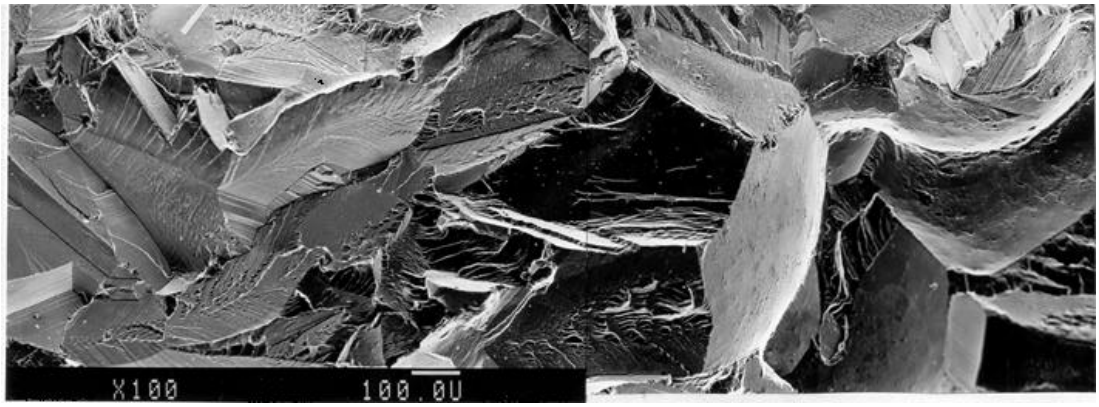

Figure 10. Crack surface of peak-aged Al-Zn-Mg polycrystal with crystallographic (111) facets and intergranular areas (high vacuum, R=0.1 and 35 Hz)

ENVIRONMENTALLY INFLUENCED FATIGUE CRACK PATH

Following the initial work of Bradshaw and Wheeler [20], the deleterious effect of ambient air on fatigue crack propagation as compared to an inert environment like high vacuum, has been clearly related to the presence of moisture in the surrounding environment for Aluminum alloys fatigued at room temperature [4, 6, 7, 8, 9, 19, 21, 22]. The main difficulty encountered to understand the role of water vapor resides in the complex interactions of an active environment with other parameters which influence the propagation, including intrinsic parameters as alloy composition and microstructure or extrinsic parameters as loading conditions, specimen geometry, crack depth, crack closure and temperature.

To document the problem of the atmospheric environment assistance, studies were conducted on the influence of gaseous moist environments on fatigue crack propagation at mid and low rates on various aluminum alloys including the high purity Al-Zn-Mg alloy studied in high vacuum. Following the framework established for the intrinsic fatigue crack propagation with the three different transgranular crack propagation stages, similar rationalization of FCG in air would be expected after correction for crack closure and Young modulus effects.

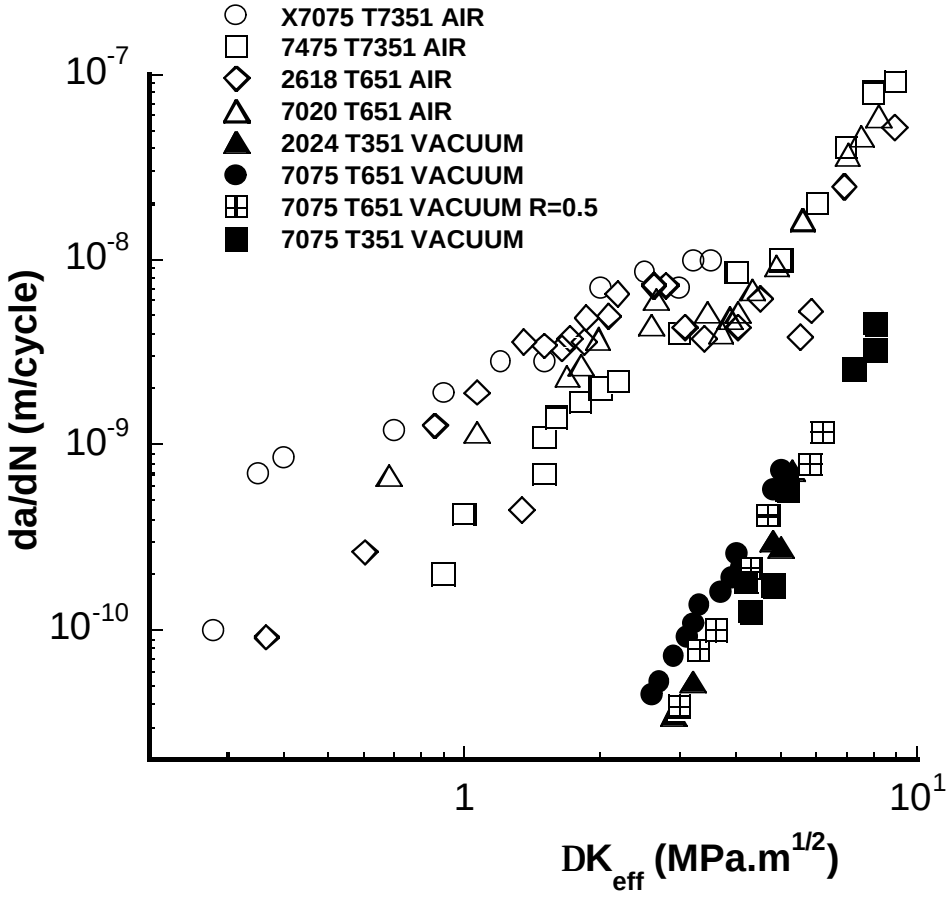

Figure 11. Effective stage II crack propagation in air and in high vacuum for a selection of Al alloys.

Figure 11 presents a compilation of stage II propagation data obtained in ambient air and in high vacuum for a selection of alloys. In accordance with the results presented here above, a remarkable rationalization of the intrinsic propagation data in high vacuum is observed, this intrinsic stage regime being described by relation (1). In

contrast, there is obviously no rationalization in air, particularly in the near-threshold domain. The sensitivity to atmospheric environment of the growth rate and of the effective threshold range is shown strongly dependent as on base metals, addition elements, and microstructures (see 7X75 alloys of different purity and aging conditions).

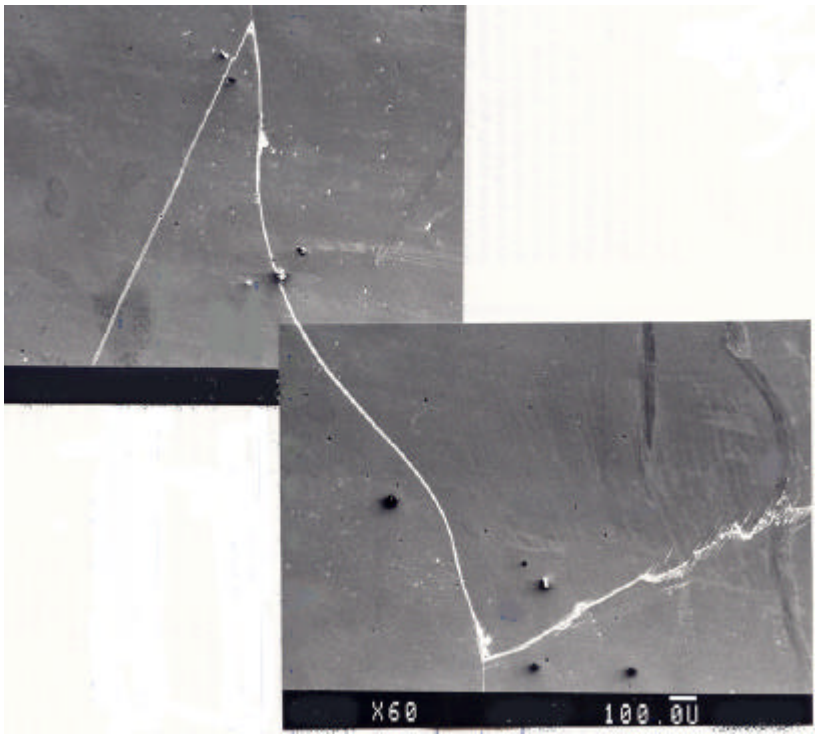

Figure 12. Crack path in a peak-aged Al-Zn-Mg bicrystal tested in air at R=0.1 and 35 Hz: stage I at low ΔK range (< 5 MPa$\sqrt{m}$), intergranular propagation when the crack meet the grain boundary and transgranular stage II crack at high ΔK range (> 10 MPa$\sqrt{m}$).

The pure environmental crack growth enhancement, which means in conditions without interaction with closure effects (oxidation, wedging, limited water vapor transport), has been analyzed by comparing effective data in gaseous environment containing well-controlled amount of water vapor and oxygen, to intrinsic data obtained in comparable loading conditions for a wide range of metallic alloys including Al, Ti and Fe based materials [4].The following conclusions have been drawn [4]:

(i) The effective propagation in ambient air is characterized in most cases by a strong environmental enhancement of the crack growth, especially near the threshold,

and is much more accentuated for Al alloys than for steels and Ti alloys at room temperature.

(ii) Ambient air as well as humid gaseous environments favor stage II propagation in most cases and in a wide range of growth rates including near-threshold conditions. In contrast to the intrinsic stage II, environmentally-assisted effective stage II is highly sensitive to several factors including alloy composition, microstructure, grain size and yield strength.

An illustration of the path of a crack grown in air in a bicrystal at R=0.1 and 35 Hz is given in Fig. 12. Depending on the stress level, the orientation of the slip system and of the boundary with respect to the load axis, the crack path can be transgranular (stage I or stage II) or intergranular. As in high vacuum, low stress level, underaged condition and easy slip orientation favor transgranular stage I crack path, while high stress, overaged condition and non easy slip orientation favor transgranular or/and intergranular crack path.

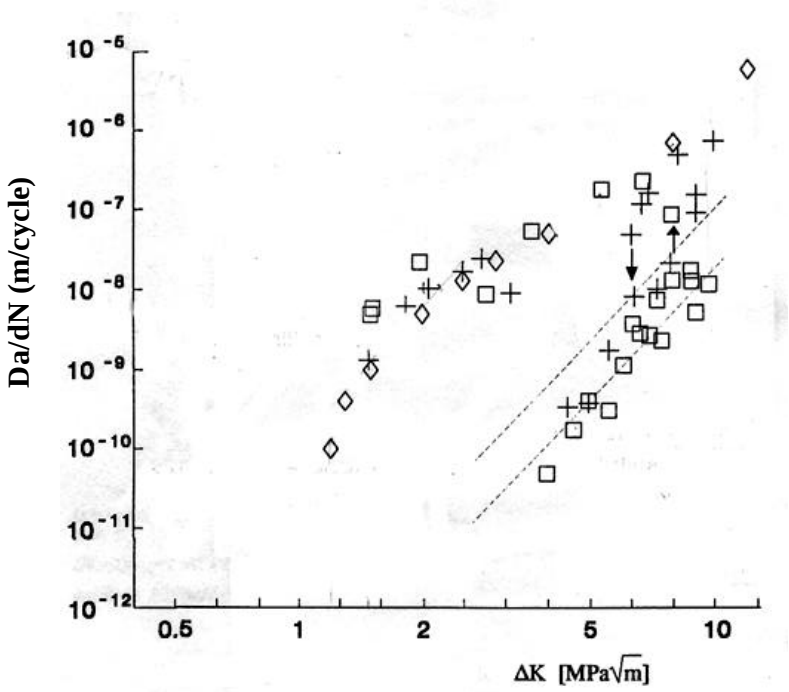

Figure 13. Crack propagation data in air and in high vacuum in a bicrystal of Al-Zn-Mg high purity alloy : i) + : air → vacuum test at 35Hz and R=0.1(↓ indicate the transition from air to high vacuum); ii) ÿ : vacuum → air test at 35Hz and R=0.1 (↑ indicate the transition from vacuum to air); iii) : intergranular propagation in air at 35Hz and R= -1 ($\Delta K=K_{max}$).

However, three major differences between air and vacuum must be underlined [4] : i) the crack growth rates in air are faster for all the crack propagation stages, ii) gas molecules adsorption on fresh cracked surfaces will promote activation of secondary slip systems and hence favor the occurrence of a stage II propagation, and iii) the effective threshold in air is much lower than in high vacuum.

The corresponding da/dN vs ΔK diagrams are plotted in Fig. 13. The crack growth rate in air is 100 times faster than in vacuum at ΔK ranges of 4 to 5 MPa$\sqrt{m}$, and the threshold ΔK_{th} is ~ 1.3 MPa$\sqrt{m}$ in air compared to ~ 4 MPa$\sqrt{m}$ in vacuum. At higher ΔK in the mid rate range the influence of environment is still there but much less important.

Such behavior has been analyzed as the superimposing of two distinct processes [4]:

(i) Adsorption of water vapor molecules which promotes the growth process without altering the basic intrinsic mechanism of damage accumulation. Adsorption of gaseous species onto fresh surfaces (Rhebinder effect [21]) is analyzed as a decrease in the critical cumulated displacement D* described in term of the surface coverage coefficient θ [4]. This regime is generally operative in the mid rate range at atmospheric pressure, and can be active for near-threshold conditions at sufficiently low pressure or/and by lowering the test frequency.

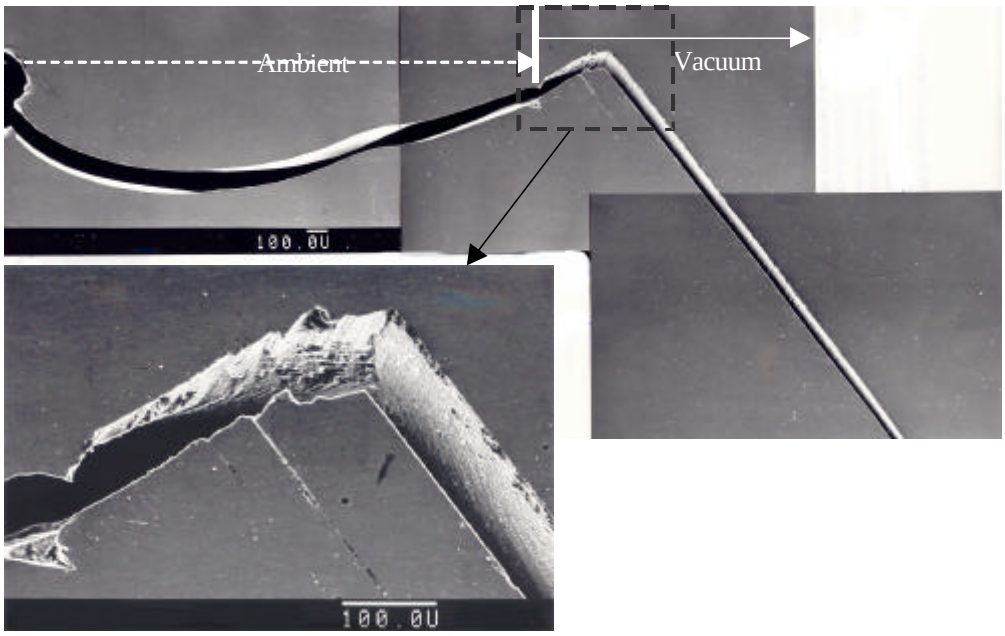

Figure 14. Crack profile in a bicrystal: i) crack initiation and propagation in ambient within the grain boundary; ii) transition from intergranular stage II to transgranular stage I in vacuum after 300 µm of intergranular propagation.

(ii) Hydrogen-assisted propagation as initially described by Wei and co-authors [6] in which hydrogen is provided by the dissociation of adsorbed water vapor molecules and is then dragged by mobile dislocations into the highly plastically strained material ahead of the crack tip where the very embrittling reaction takes place. Critical conditions for such embrittling process would thus correspond to the kinetics of the reaction and its dependence on parameters such as water vapor pressure, time (frequency) and temperature. This regime is generally observed in near-threshold conditions, at growth rate below a critical step ranging about 10^{-8} m/cycle which corresponds to stress intensity factor ranges at which the plastic deformation becomes localized within each individual grain along the crack front.

Another illustration of the influence of environment is given is Fig. 14. A crack was initially grown in air within a grain boundary of a bicrystal of the peak-aged alloy. When environment is switched to high vacuum, in first step the crack continues to follow the grain boundary; but in second step the crack suddenly changes to a transgranular path within a (111) plane which appears to be the preferential path in the inert environment.

This experiment illustrates three characteristic features of the fatigue crack propagation assisted by the atmophere environment: i) atmospheric environment favors intergranular crack path, ii) the size of the first step of propagation in vacuum following the intergranular propagation in air demonstrates an embrittlement of the process zone ahead of the crack tip which extend of about 300µm for an applied ΔK range of 5.7 MPa$\sqrt{m}$; iii) the strain localization is reduced by ambient air since gas adsorption favors the activation of secondary slip systems, and hence promotes the stage II propagation regime.

CONCLUSIONS

From this overview of the influence of environment and of microstructure on the near-threshold fatigue crack path in Aluminum alloys, the following conclusion can be drawn:

1) Four characteristic intrinsic crack propagation regimes have been identified on single crystals and bicrystals and polycrystals of high purity Al-Zn-Mg alloys and 7XXX commercial alloys tested in high vacuum in condition without closure or with closure correction. Typical crack paths have been associated to these intrinsic propagation corresponding to stage I, stage II and stage I like transgranular regimes and toone intergranular regime. The condition for the occurrence of the different crack propagation mechanisms and their associated paths have been analyzed with respect to aging conditions and corresponding microstructures.
2) The influence of the ambient atmosphere on the same materials and in comparable testing conditions as in high vacuum has been shown: (i) to accelerate the crack propagation in air for the four crack growth regimes, (ii) to reduce drastically the

effective threshold range of the stress intensity factor in air, and iii) to favor intergranular propagation and stage II transgranular crack propagation in air.

REFERENCES

1. Backlund, J., Blom, A. F. and Beevers, C. J. (1982) *Fatigue Thresholds,* EMAS Pub.
2. Davidson, D. L. and Suresh, S. (1984) *Fatigue Crack Growth Threshold Concepts,* The Metallurgical Society of AIME Pub., Philadelphia, Pa, USA.
3. Newman Jr, J.C. and Piascik, R. S. (2000) *Fatigue Crack Growth Threshold, Endurance Limits and Design, ASTM STP 1372*, American Society for Testing and Materials Pub., Philadelphia.
4. Petit, J., Hénaff, G. and Sarrazin-Baudoux, C. (2000) *ASTM STP 1372*, 3-30
5. Newman Jr., J. C. and Elber, W. (1988) *Mechanics of Fatigue Crack Closure,* ASTM STP 982, American Society for Testing and Materials Pub., Philadelphia, Pa, USA.
6. Wei, R. P. (1968) *Engineering Fracture Mechanics* **1**, 633-651.
7. Elber, W. (1971) *ASTM STP 486*, 230-242
8. Petit, J. (1983) In: *Fatigue Crack growth Thresholds Concepts,* pp. 3-25, Davidson, D. and Suresh, S. (Eds), TMS AIME pub., Philadelphia, Pa, USA.
9. Petit, J., Kosche, K. and Gudladt, H. J. (1992) *Scripta metall mater* **26**, 1049-1054.
10. Kosche, K. (1991) Phd Thesis, University of Stuttgart.
11. Petit, J. and Zeghloul, A.(1989) *Revue Phys. Appl.* **24**, 905-913.
12. Petit, J. and Zeghloul, A. (1990) *ASTM-STP 1049*, 334-346.
13. Petit, J. and Hénaff, G. (1991) *Scripta Metall.* **25**, 2683-2687.
14. Rice, J. R.(1965) In : *Proceeding of International Conference on Fracture,* Sendaï Japan, pp. 283-308.
15. Weertman, J. (1966) *International Journal of Fracture Mechanics* 2, 460-467.
16. Suresh, S. (1985) *Metallurgical Transactions* 16A, 249-260.
17. de Los Rios, E. R., Mohamed, H. J. and Miller, K. (1985) *Fatigue & fracture of Engineering Materials and Structures* 8, 49-63.
18. Pelloux, R. M. N. (1970) *Engng Fract Mech* **1**, 697-704.
19. Davidson, D. L. and Lankford, J. (1983) *Fat Engng Mater Struct* **3** , 241-256.
20. Bradshaw, F. J. and Wheeler, C. (1966) *Applied Materials Research* 112-120.
21. Bouchet, B., de Fouquet, J. and Aguillon, M. (1975) *Acta Met* **23,** 1325-1336.
22. Piascik, R. S. and Gangloff, R. P. (1991) *Metall Trans* **22A,** 2415-2428.